INORGANIC CHEMISTRY

FRONTIERS

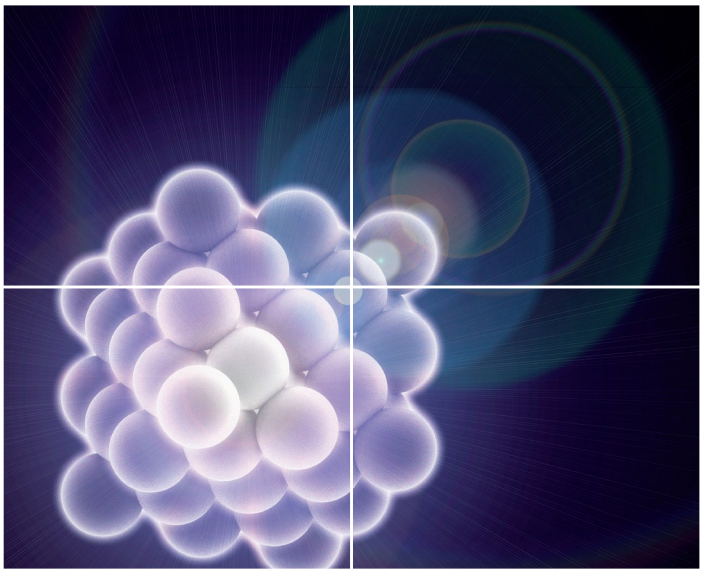

Accepted Manuscript

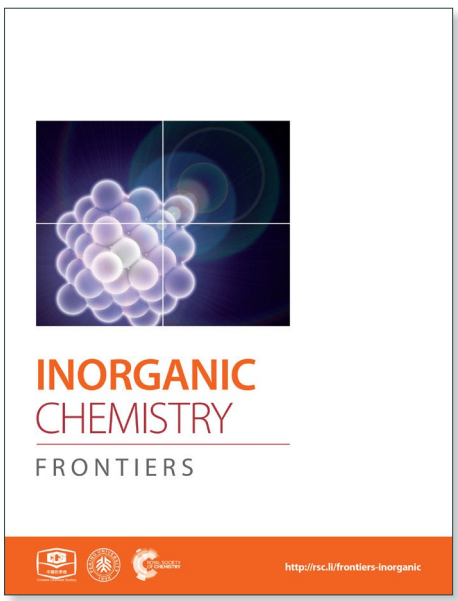

This is an *Accepted Manuscript*, which has been through the Royal Society of Chemistry peer review process and has been accepted for publication.

Accepted Manuscripts are published online shortly after acceptance, before technical editing, formatting and proof reading. Using this free service, authors can make their results available to the community, in citable form, before we publish the edited article. We will replace this *Accepted Manuscript* with the edited and formatted *Advance Article* as soon as it is available.

You can find more information about *Accepted Manuscripts* in the **Information for Authors**.

Please note that technical editing may introduce minor changes to the text and/or graphics, which may alter content. The journal's standard **Terms & Conditions** and the **Ethical guidelines** still apply. In no event shall the Royal Society of Chemistry be held responsible for any errors or omissions in this *Accepted Manuscript* or any consequences arising from the use of any information it contains.

Journal Name

ARTICLE

The effect of magnetic coupling on magneto-caloric behaviour in two 3D Gd(III)-glycolate coordination polymers

Received 00th January 20xx,
Accepted 00th January 20xx

DOI: 10.1039/x0xx00000x

www.rsc.org/

Jiang-Zhen Qiu,[a] Yan-Cong Chen,[a] Long-Fei Wang,[a] Quan-wen Li,[a] Martin Orendáč,[b] and Ming-Liang Tong,*[a]

Two different 3D coordination polymers, $[Gd(glc)(Hglc)(H_2O)]_n \cdot nH_2O$ (**1**) and $[Gd(Hglc)_3]_n$ (**2**) (H_2glc = glycolic acid), have been prepared based on the reaction of Gd(III) ions with H_2glc in different pH environment. Due to the deprotonation of the α-OH groups from a half of H_2glc ligands in **1**, the $[Gd_2]$ units with the Gd-O-Gd bridging model are observed and suggest a stronger magnetic coupling than that in **2**. Magnetic and heat capacity studies reveal the significant impact of the strength of magnetic coupling on the magneto-caloric effect (MCE) in systems. Although a theoretical calculation suggests the $-\Delta S_m$ (50.5 J kg^{-1} K^{-1}) of **1** is larger than **2** (45.2 J kg^{-1} K^{-1}), the stronger antiferromagnetic coupling in **1** decrease the number of low lying spin ground states upon the lowering of temperature, thus giving a smaller value of $-\Delta S_m$ than **2** at various fields (eg. $-\Delta S_{m,max}$ = 24.8 J kg^{-1}K^{-1} and 41.1 J kg^{-1}K^{-1} for **1** and **2** respectively at ΔH = 3 T). This case reveals that the effect of magnetic coupling on MCE plays a dominant role for designing low-temperature 3D Gd(III)-based magnetic coolants.

Introduction

The magnetocaloric effect (MCE), which was firstly observed in metallic iron in 1881 by Warburg, is dependent on the change of magnetic entropy upon application of a varying magnetic field.[1] Such interesting phenomenon could be used in cooling applications via adiabatic demagnetization. In recent years, the molecular magnetic refrigerators working at low temperature region with large MCE attracted intense interests of researchers due to its obvious merits, eg. energy-efficiency, economy, environmental friendly nature, synthetic controllability and functional tunability, in contrast to traditional refrigerators.[2] Theoretically, the magnetic coolants will possess a large entropy change ($-\Delta S_m$) when meeting some conditions: (1) a large spin ground state S due to the magnetic entropy amount to $R\ln(2S+1)$;[3] (2) a small magnetic anisotropy can hinder the polarization of net molecular spins along the easy axis;[4] (3) a high magnetic density (or a large metal/ligand mass ratio), since the diamagnetic ligands have negative impact on MCE;[5] (4) a weak magnetic coupling in magnetic coolant will results in a lower working temperature and a maxima of $-\Delta S_m$ close to its paramagnetic limit.[6]

Therefore, the combination of light ligands and Gd(III), which has a large spin value (S = 7/2) and is isotropy, and has been proven as one of the effective strategies for obtaining magnetic coolers with a large MCE. To date, a large number of Gd(III) based molecular clusters and coordination polymers with impressive MCE are reported.[5,7,8,9] Among them, the construction of high-dimensional Gd(III) based polymers, such as $[Gd(HCOO)(OAC)_2(H_2O)_2]_n$,[9a] $[Gd(HCOO)_3]_n$,[9b] $[Gd(OH)CO_3]_n$,[9c] and $[GdF_3]_n$,[8f] is beneficial to obtain the materials with promising MCE, when considering the enhanced magnetic density due to the sharing of bridging ligands between magnetic centers and that the nonmagnetic guest or solvent molecules are more difficult to be trapped in such structures.

On the other hand, as the increasing magnetic density in systems, the distance between the Gd(III) ions will be shorter, which may result in stronger magnetic superexchange-coupling. Although the magnetic coupling between Gd(III) ions is weak due to the shielding effect of 5s and 5p orbitals, however, the strengthening of magnetic coupling, which may results in higher ordering temperature,[10] is unfavorable for magnetic coolers working at lower temperature, especially in ultra-low temperature region (i.e., sub-millikelvin).

Herein, we report a family of 3D coordination polymers, $[Gd(glc)(Hglc)(H_2O)]_n \cdot nH_2O$ (**1**) and $[Gd(Hglc)_3]_n$ (**2**) (H_2glc = glycolic acid). The structural analysis indicates the α-OH groups of a half of H_2glc ligands in **1** are deprotonated, giving

[a] *J.-Z. Qiu, Y.-C. Chen, L.-F. Wang, Q.-W. Li, Prof. Dr. M.-L. Tong*
Key Laboratory of Bioinorganic and Synthetic Chemistry of Ministry of Education
School of Chemistry & Chemical Engineering
Sun Yat-Sen University
Guangzhou, 510275 (P. R. China)
Fax: (+)86 20 8411-2245
E-mail: tongml@mail.sysu.edu.cn
[b] *prof. Dr. Martin Orendáč*
Centre of Low Temperature Physics Faculty of ScienceLaboratory
Institute of Experimental Physics SAS
P. J. Šafárik University
Park Angelinum 9, 04013 Košice, Slovakia
E-mail: martin.orendac@upjs.sk

† Footnotes relating to the title and/or authors should appear here. Electronic Supplementary Information (ESI) available: [details of any supplementary information available should be included here]. See DOI: 10.1039/x0xx00000x

di-deprotonated glc^{2-} anions, while only the mono-deprotonated $Hglc^-$ anions, as a result of deprotonation of the carboxyl groups of H_2glc, are observed in **2**. Although the antiferromagnetic (AF) couplings are found in both complexes, however, the different degree of deprotonation of H_2glc leads to various strength of magnetic couplings in **1** and **2**. For **1**, each deprotonated hydroxyl oxygen atom bridges two Gd(III) ions into a $[Gd_2]$ unit, leading to a stronger intra-dinuclear AF coupling than **2**, in which the Gd(III) ions are more seperated with a Gd-OCO-Gd connecting model (Scheme 1), thus giving a very weak magnetic coupling. As confirmed by the MCE measurements, although the theoretical maxima $-\Delta S_m$ of **1** (50.5 J $kg^{-1}K^{-1}$) is larger than **2** (45.2 J kg^{-1} K^{-1}), the relatively strong AF coupling in **1** decrease the number of low-lying excited spin states, resulting in a weaker MCE ($-\Delta S_{m,\,max}$ = 40.7 J $kg^{-1}K^{-1}$, $\Delta T_{ad,\,max}$ = 16 K at ΔH = 7 T) than **2** ($-\Delta S_{m,max}$ = 43.7 J $kg^{-1}K^{-1}$, $\Delta T_{ad,max}$ = 24.5 K at ΔH = 7 T). Additionaly, at the lower temperature down to 0.5 K at ΔH = 7 T, the $-\Delta S_m$ of **2** still maintain a considerable value of 39.5 J $kg^{-1}K^{-1}$, which is obviouly higher than that of **1** ($-\Delta S_{m,max}$ = 17.1 J $kg^{-1}K^{-1}$), confirming the weak magnetic coupling in **2** make it as a promising magnetic refrigerator working at low temperature.

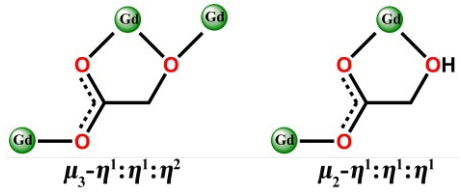

Scheme 1. The bridging model of di-deprotonated glc^{2-} (left) and mono-deprotonated $Hglc^-$ ligand (right) with Gd(III) ions.

Experimental

Synthesis: All chemicals were obtained from commercial sources and used as received without further purification.

$[Gd(glc)(Hglc)(H_2O)]_n \cdot nH_2O$ (1): A mixture of $Gd(acac)_3 \cdot 3H_2O$ (51mg, 0.1mmol) and Hglc (30 mg, 0.4 mmol) was dissolved in 10 ml H_2O/MeOH (V:V = 1:1) followed by the addition of $[(CH_3)_4N]OH \cdot 5H_2O$ (0.009g, 0.05 mmol). The resulting solution was resealed in a Teflon-lined, stainless steel vessel (23 mL) and heated at 120 °C for 3 days, and then cooled to room temperature at a rate of 5°C/h. Colorless block crystals (yield: 81%) were obtained. Elemental analysis (%) calc for $C_4H_9GdO_8$: C 14.03, H 2.65; found: C 13.90, H 2.68. Infrared (KBr disc, cm^{-1}): 3599 (m), 3448 (m), 3276 (m), 3140 (m), 2889 (m), 2827 (m), 2640 (m), 2440 (w), 2214 (w), 2106 (w), 1599 (s), 1545 (s), 1410 (s), 1227 (w), 1105 (s), 1057 (s), 1005 (w), 937 (m), 716 (m), 575 (m), 530 (m), 467 (m), 277 (m).

$[Gd(Hglc)_3]_n$ (2): A mixture of $Gd(acac)_3 \cdot 3H_2O$ (51mg, 0.1mmol) and H_2glc (30 mg, 0.4 mmol) in 10 ml solution of H_2O/MeOH (V:V = 1:1) was resealed in a Teflon-lined, stainless steel vessel (23 mL) and heated at 120 °C for 3 days, and then cooled to room temperature at a rate of 5°C/h. Colorless block crystals (yield: 60%) were obtained. Elemental analysis (%) calcd for $C_6H_9GdO_9$: C, 18.84，H 2.37; found: C 18.61, H 2.49. Infrared (KBr disc, cm^{-1}): 3395 (br), 2948 (m), 2813 (w), 2659 (w), 1590 (vs), 1475(w), 1448 (w), 1403 (m), 1385 (s), 1333 (s), 1332 (w), 1080 (s), 1064 (s), 998 (w），940 (m), 817 (w), 707 (m), 575 (w), 540 (m).

General characterization: Elemental analyses were performed on an Elementar Vario EL elemental analyzer. Powder X-ray diffraction measurements (Fig. S1, ESI†) were performed with a Bruker D8 X-Ray Diffractometer. The FTIR spectra were measured on a Thermo NICOLET AVATAR 330 FTIR spectrometer.

Crystal data: Crystal diffraction data was recorded at 150(2) K on a Rigaku R-AXIS SPIDER Image Plate Diffractometer with MoKa radiation. The structures were solved by direct methods and all nonhydrogen atoms were refined anisotropically by least square on F^2 using the SHELXTL program[11].

For 1: $C_4H_9GdO_8$, M_r = 342.36, monoclinic, space group $P2_1/c$, a = 6.2789(3) Å, b = 9.0295(6) Å, c = 14.8336(9) Å, α = 90°, β = 92.585(2)°, γ = 90°, V = 840.14(9) $Å^3$, Z = 2, ρ = 2.707 g cm^{-3}; R_1 = 0.0292 ($I > 2\sigma(I)$), wR_2 = 0.0729 (all data). Final *GooF* = 1.035.

For 2: $C_6H_9GdO_9$, M_r = 382.38, monoclinic, space group $P2_1$, a = 8.1242(11) Å, b = 8.0394(13) Å, c = 8.4324(12) Å, α = 90°, β = 117.490(4)°, γ = 90°, V = 488.57(13) $Å^3$, Z = 2, ρ = 2.599 g cm^{-3}; R_1 = 0.0423 ($I > 2\sigma(I)$), wR_2 = 0.1001 (all data). Final *GooF* = 1.099.

CCDC 1426346 (**1**) and 1426347 (**2**) contain the supplementary crystallographic data for this paper. These data can be obtained free of charge from the Cambridge Crystallographic Data Centre via www.ccdc.cam.ac.uk/data_request/cif.

Magnetic measurements: The magnetic measurements were performed by using a Quantum Design MPMS XL-7 SQUID magnetometer and a Quantum Design PPMS on polycrystalline samples with an empirical diamagnetic correction. The specific heat was studied in a Quantum Design PPMS with the ^{3}He option adopting standard relaxation technique.

Results and discussion

Both complexes are synthesized through a hydrothermal process of Gd^{3+} and H_2glc in H_2O/MeOH solution. The presence of tetramethylammonium hydroxide is essential for separating complexes **1** and **2**, for which the α-OH group of H_2glc could be deprotonated in an alkaline environment, thus giving the di-deprotonated glc^{2-} ligand. Besides, the acetylacetonate (acac) may serve as an auxiliary ligand to prevent the hydrolysis of Gd^{3+} ions into other compounds.[7a]

Single-crystal X-ray diffraction analysis reveals complex **1** crystallize in monoclinic $P2_1/c$ space group with one full formula unit in the asymmetric unit cell. In the crystal structure, each Gd(III) center is coordinated by eight oxygen atoms from two mono-deprotonated $Hglc^-$ ligands, three di-deprotonated glc^{2-} ligands and one water molecule, resulting in the Triangular dodecahedron geometry (Fig. 1) with the *CShM* value of 0.79 calculated by SHAPE 2.1.[12] The Gd-O bond lengths range from 2.283(3) to 2.521(3) Å.

Both $Hglc^-$ and glc^{2-} ligands are observed in the structure of **1** and employing μ_3-η^1:η^1:η^2 and μ_2-η^1:η^1:η^1 bridging modes

respectively between the Gd(III) ions (Scheme 1). Upon the bridging of the hydroxyl μ_2-oxygen atoms from glc^{2-} ligands between two Gd(III) ions, the [Gd_2] dinuclear units are formed and connected with each other through four glc^{2-} ligands, extending to a 4-connected 2D layer on the *bc* plane of unit cell (Fig. 2a-b). The Gd(III) ions in dinuclear unit are separated with 3.7880(3) Å and the Gd-O-Gd angle is 110.37(11)°. Additionally, the [Gd_2] dinuclear units in the 2D layers are bridged by $Hglc^-$ ligand along *a* axis of unit cell, forming a 3D structures with a typical *pcu* topology (Fig. 2c-d).

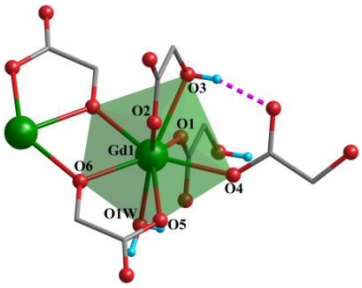

Fig. 1 The coordination environments of Gd(III) in complex **1**. The hydrogen bonds are displayed as purple dashed lines. Color codes: Gd (green), O (red), C (gray) and H (blue). For clarity, the hydrogen atoms on methylene are omitted.

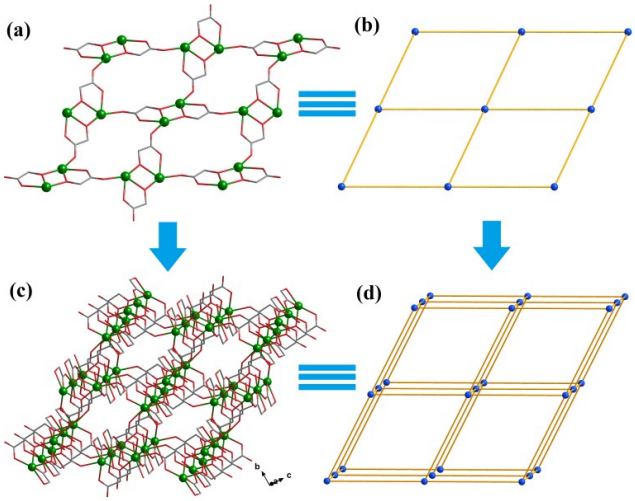

Fig. 2 The 2D layer constructed by [Gd_2] dinuclear units and glc^{2-} ligands (a) and its simplified structure (b); The extended 3D structure of **1** (c) bridged by $Hglc^-$ between layers and its simplified topological structure (d). Blue spheres represent [Gd_2] dinuclear units as 6–connected nodes.

Complex **2**, which is synthesized in the absence of tetramethylammonium hydroxide, crystallizes in the monoclinic space group $P2_1$. The asymmetric unit of **2** contains one Gd(III) ion and three mono-deprotonated $Hglc^-$ ligands. In contrast with **1**, only mono-deprotonated $Hglc^-$ ligands are observed in **2**, indicating the degree of deprotonation of H_2glc is pH-dependent and thus making the "fine-tuning" of the coordinating structure possible. In **2**, each $Hglc^-$ ligand not only chelates a Gd(III) ion with the carboxyl and hydroxyl groups, but also extends into a μ-bridging mode by an *syn–anti* carboxyl bridge (Gd-OCO-Gd, 6.3784(11) Å). As far as Gd(III) is concerned, each Gd(III) ion is coordinated with nine oxygen atoms from six $Hglc^-$ ligands, giving a spherical capped square antiprism geometry with *CShM* value of 0.59. More precisely, three of the ligands chelate the Gd(III) center with two oxygen atoms from hydroxyl and carboxylic group respectively, whereas the other three ligands are coordinated in the opposite direction through one carboxyl oxygen atom (Fig. 3). Topologically, the Gd(III) ions can be simplified as 6-connected nodes (Fig. 4a-b) and the ligands as linkers, which gives rise to a 3D *acs* topology (Fig. 4c-d).[13]

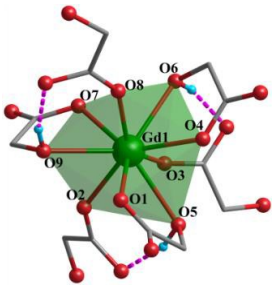

Fig. 3 The coordination environments of Gd(III) in complex **2**.

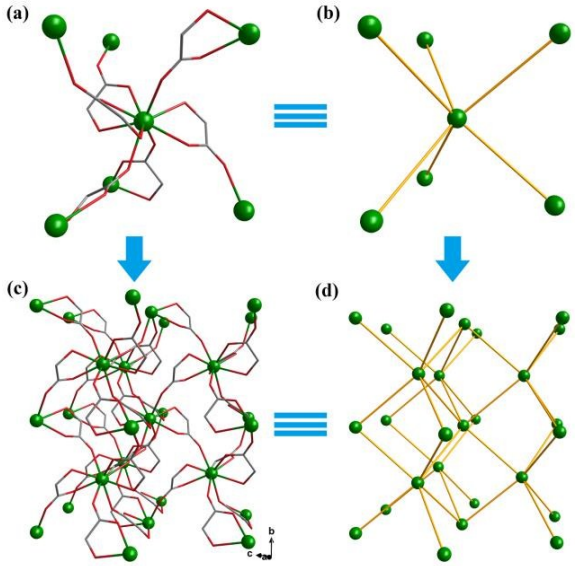

Fig. 4 Each Gd(III) ion is connected with six other Gd(III) ions through the bridging $Hglc^-$ ligands (a) and can be simplified as a 6-connected node (b), so the 3D structure of **2** (c) could be simplified as a 3D *acs* topology (d).

The variable-temperature magnetic susceptibilities of **1** and **2** were collected from 1.8 to 300 K and 2 to 300 K for **1** and **2** respectively in an applied direct-current (dc) field of 0.1 T. At room temperature, the $\chi_m T$ values for complexes **1** and **2** are 7.87 cm^3 K mol^{-1} and 7.84 cm^3 K mol^{-1}, respectively, which are both in good agreement with the spin-only value expected for a free Gd(III) ion with g = 2 (7.875 cm^3 K mol^{-1}). However, as the decreasing of temperature, both complexes exhibit different magnetic behaviours. For **1**, the $\chi_m T$ value remains essentially constant upon lowering of the temperature to about 30 K, after which it decreases sharply to a minimum value of 2.85 cm^3 K mol^{-1} at 1.8 K (Fig. 5a), indicating AF coupling in

1, which is in agreement with the Curie-Weiss fitting for **1** (C = 7.94 cm^3 mol^{-1} K and θ = -2.07 K). The $\chi_m T$ value for **2** is essentially constant, between 7.51 and 7.84 cm^3 K mol^{-1}, with very weak interactions as indicated by the Curie-Weiss fit (C = 7.85 cm^3 K mol^{-1}, θ = -0.6 K in the range 1.8-300 K, Fig. 5b). For further understanding the magneto-structural correlations of both complexes,[14,15] the fitting of the variable-temperature magnetic susceptibilities and magnetization of **1** and **2** was performed using PHI software.[16] For **1**, the dominant antiferromagnetic interaction is inside the [Gd_2] dinuclear unit with J = -0.103 cm^{-1}, accompanied by a negligible zJ < 0.001 cm^{-1}. For **2**, the antiferromagnetic interaction can be easily rationalized by an intermetallic zJ = -0.005 cm^{-1} (Fig. 5). It is obviously the AF interactions in **1** are stronger than **2**, such observation is mainly attributed to the single-oxygen bridged Gd(III)···Gd(III) coupling in the [Gd_2] unit of **1**, in which the Gd(III)···Gd(III) distance (3.7880(3) Å for **1**) is obviously shorter than **2** (6.3036(6) Å), resulting in stronger AF coupling in **1**.[17]

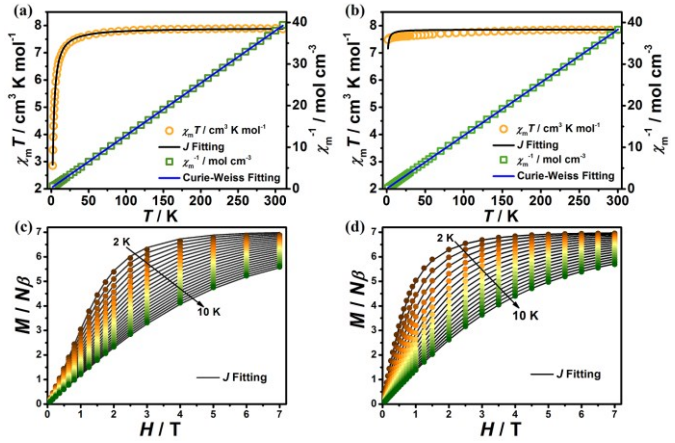

Fig. 5 Temperature-dependencies of the magnetic susceptibility products, $\chi_M T$, and the inverse magnetic susceptibilities, $1/\chi_M$, at 1.8-300 K with a dc field of 0.1 T for complexes **1** (a) and **2** (b). Field-dependencies of the magnetization for **1** (c) and **2** (d) at 2-10 K. The solid lines represent the magnetic coupling parameter (J) (black) and Curie-Weiss (blue) fitting, respectively.

Magnetization measurements were performed at T = 2-10 K for **1** and **2**, in the field range of 0.01-7 T (Fig. 5c,d). The magnetization increase steadily with the external field and reach the saturation values 6.90 and 7.02 $N\beta$ for **1** and **2** respectively at 1.8 K and 7 T, which are in good agreement with the theoretical value of 7 $N\beta$ for a Gd(III) ion (S = 7/2, g = 2).

According to experimental magnetization data, the magnetic entropy changes (-ΔS_m) for **1** and **2** can be calculated by applying the Maxwell equation.[18]

$$\Delta S_m = \int_0^H [\partial M(T,H)/\partial T]_H dH$$

The magnetic field dependent magnetic entropy change (-ΔS_m) of each complex at various temperatures is shown in Fig. 6. It is obviously observed that the -ΔS_m values of **1** and **2** gradually increase with the lowering of temperature and increasing of applied fields. For **1**, the -ΔS_m value reaches a maxima value of 40.7 J kg^{-1}K^{-1} with ΔH = 7 T at 2 K (Fig. 6a), which is far smaller than its theoretical limiting value of 50.5 J kg^{-1}K^{-1} calculated from Rln(2S_{Gd} + 1) with S_{Gd} = 7/2. For **2**, due to the relatively smaller metal/ligand ratios of **2** in contrast to **1**, the calculated theoretical maximum -ΔS_m with the value 45.2 J kg^{-1} K^{-1} is smaller than that of **1**, however, the experimental result indicates the MCE effect for **2** is more promising than **1**, as confirmed by the larger -ΔS_m with the experimental value of 43.7 J kg^{-1}K^{-1} at T = 2 K and ΔH = 7 T (Fig. 6b). Such observation mainly origin from the different strength of magnetic coupling in these two systems as confirmed by their different magnetic coupling parameters (J). As a result, the obvious antiferromagnetic coupling in **1** can decrease the number of low lying spin states upon the lowering of temperature, leading to the decreasing of magnetic entropy changes while the magnetic coupling in **2** is much weaker, make the Gd(III) ions keep mainly paramagnetic states at lower temperature and give a large MCE close to its paramagnetic limits. The volumetric -ΔS_m for **1** and **2** are 107.7 and 113.6 mJ cm^{-3} K^{-1} respectively. Both **1** and **2** display considerable MCE in comparison with some reported 4f magnetic coolants in Table 1.

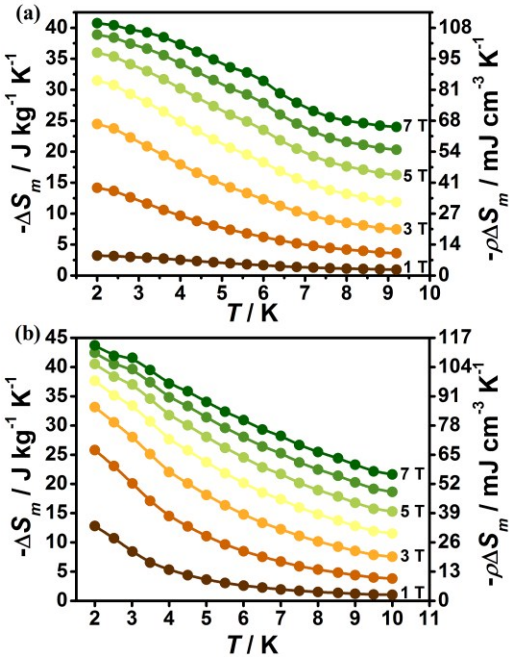

Fig. 6 Magnetic entropy changes obtained from the magnetization data for **1** (a) and **2** (b).

Heat capacity

To further investigate MCE of **1** and **2**, the low-temperature heat capacities (C) measurements were performed at applied fields of 0, 3, 5 and 7 T down to approximately 0.5 K. As shown in Fig. 7, the higher temperature regions for the two complexes are dominated by lattice contributions arising from the thermal vibration, which fit well to the Debye's model and yield the Debye temperature (Θ_D), 272 and 460 K for **1** and **2**

respectively. At lower temperatures, the heat capacities for the two complexes are dominated by the field-sensitive Schottky-type magnetic contributions. The observed increase of C upon cooling is attributed to calculated Schottky anomaly, however, no obvious λ peaks is found in the measured temperature range at zero field, indicating the absence of magnetic ordering for both complexes above 0.5 K.

Table 1 Magnetic entropy change for selected 4f-based magnetic coolants.

Complex	ΔH (T)	$-\Delta S_{m,max}$ J kg^{-1} K^{-1}	$-\Delta S_{m,max}$ mJ cm^{-3} K^{-1}
1 (this work)	7	40.7	110
2 (this work)	7	43.7	114
$[\{Gd(OAc)_3(H_2O)_2\}_2]\cdot 4H_2O$[8a]	7	40.6	82.8
$[Gd(HCOO)(OAc)_2(H_2O)_2]_n$[9a]	7	45.9	110
$[Gd_2(N\text{-}BDC)_3(dmf)_4]_n$[9a]	7	29.0	41.2
$[Gd(HCOO)(bdc)]_n$[8b]	9	47.0	125
$[Gd_2(OH)_2(suc)_2(H_2O)]_n\cdot 2nH_2O$[7a]	7	42.8	120
$[Gd_6(OH)_8(suc)_5(H_2O)_2]_n\cdot 4nH_2O$[7a]	7	48.0	144
$[Gd(HCOO)_3]_n$[9b]	7	55.9	215.7
$\{[Gd_6O(OH)_8(ClO_4)_4(H_2O)_6](OH)_4\}_n$[8c]	7	46.6	215.6
$[Gd(C_2O_4)(H_2O)_3Cl]$[5b]	7	48.0	144
$[Gd_4(SO_4)_4(\mu_3\text{-}OH)_4(H_2O)]_n$[8d]	7	51.3	198.9
$Gd(OH)_3$[8e]	7	62.0	346
$[Gd(OH)CO_3]_n$[9c]	7	66.4	355
GdF_3[8f]	7	71.6	506

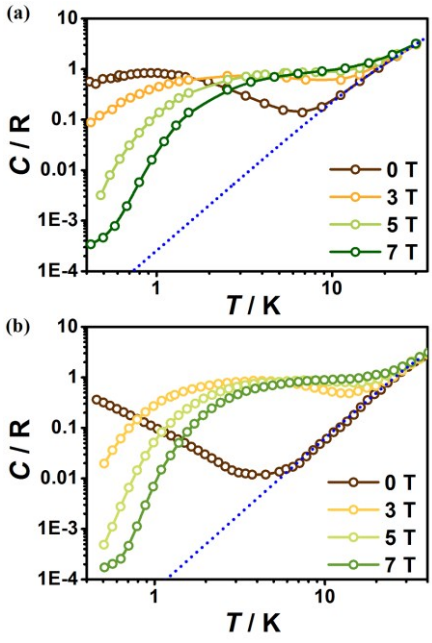

Fig. 7 Temperature dependent heat capacities (C) for **1** (a) and **2** (b) under various fields. The dotted blue lines represent the estimated lattice contribution.

From the experimental C, the temperature dependent entropies (S) for **1** and **2** are obtained by numerical integration using $S(T) = \int C(T)/T\mathrm{d}T$. Additionally, a compensation to the zero-field entropy has to be added for each complex based on the saturation value of magnetic entropy ($S_{m,sat} = R\ln(2s+1) = 2.08R$) (Fig. S2, ESI†). Therefore, the isothermal magnetic entropy change ($-\Delta S_m$) and the adiabatic temperature change (ΔT_{ad}) for each complex (Fig. 8 and 9) can be extracted from the temperature and field dependencies of the relative $S_{total}(T_0,H)$ data by vertical subtraction.

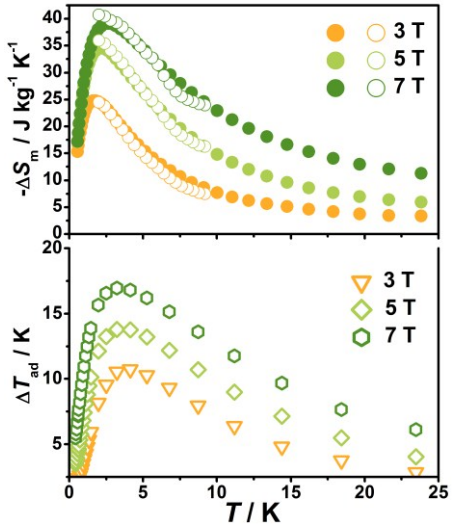

Fig. 8 Magnetic entropy change (solid circles) and adiabatic temperature change obtained from the heat capacity for **1** at various temperatures and field changes. The hollow circles represent magnetic entropy obtained from magnetization.

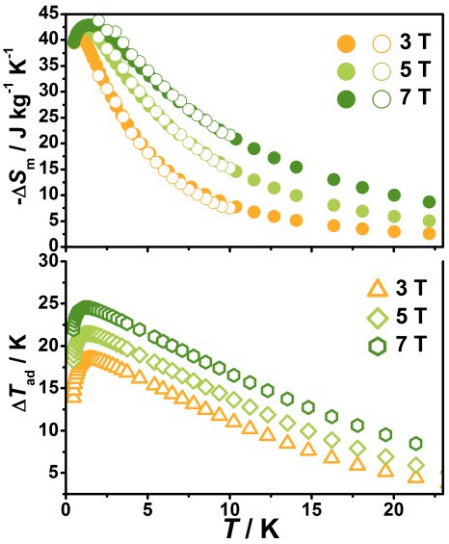

Fig. 9 Magnetic entropy change (solid circles) and adiabatic temperature change obtained from the heat capacity for **2** at various temperatures and field changes. The hollow circles represent magnetic entropy obtained from magnetization.

With the information available in the lower-temperature region, one can easily recognize the peaks of the $-\Delta S_m$-T curves and the expected shift to higher temperature with an increasing field. The ΔS_m of each complex shows good agreement from both independent evaluations, that is, heat capacity and magnetization respectively, confirming the consistency of the two measurements of magnetic entropy change. Due to the

weaker magnetic coupling in **2**, the observed peak of $-\Delta S_m$ for **2** is obviously located at lower temperature than **1**. At ΔH =7 T, the corresponding maximum of $-\Delta S_m$ for **2** is observed at 1.4 K, obviously lower than that of **1** (2.6 K). Additionally, it is noted the maximum of $-\Delta S_m$ for **2** at a mild field of ΔH = 3 T give a considerable value of 41.1 J kg^{-1}K^{-1} at 0.78 K, which is also close to its maximum of 43.7 J kg^{-1}K^{-1} at 7 T, indicating the energy efficiency and practical applicability of **2**. What's more important, as the lowering of temperature to 0.5 K, which is the lowest measured temperature, complex **2** still maintain a high $-\Delta S_m$ of 39.5 J kg^{-1}K^{-1} while the $-\Delta S_m$ of **1** sharply decreases to 17.1 J kg^{-1}K^{-1}, such observation indicates the weak magnetic coupling avoid the magnetic ordering of **2** at low temperature, thus make it a potential candidate for the ultra-low temperature application.

When considering the other parameter, ΔT_{ad}, complex **2** with the maxima of 24.5 K for ΔH = 7 T is also obviously superior to **1** (ΔT_{ad} = 16.9 K at T = 3.2 K and ΔH = 7). Such larger ΔT_{ad} of **2** in contrast to **1** is due to not only its higher $-\Delta S_m$ value, but also the higher Debye temperature of **2**, which leads to less lattice contribution of the heat capacity at the corresponding temperature, and therefore a relatively greater temperature variation can be obtained.

Conclusions

In summary, through controlling the degree of pH environment in the hydrothermal reaction of H_2glc ligands and Gd(III) ions, we successfully obtain two Gd(III)-based polymers, **1** and **2**. In the structure of **1**, due to the deprotonation of the α-OH group of H_2glc, each hydroxyl oxygen atom bridges two Gd(III) ions in μ_2 model (Gd-O-Gd, 110.37(11)°), resulting in a [Gd_2] dinuclear, thus giving a stronger magnetic coupling than **2** in which the Gd(III) ions are more separated with 6.3784(11) Å through Gd-COC-Gd bridging model. A theoretical calculation suggested higher $-\Delta S_m$ value of **1** than **2**, however, the following MCE measurement indicates both the maxima of $-\Delta S_m$ and ΔT_{ad} of **2** at ΔH = 7 T ($-\Delta S_{m,max}$ = 43.7 J kg^{-1}K^{-1}, $\Delta T_{ad,max}$ = 24.5 K) are larger than **1** ($-\Delta S_{m,\,max}$ = 39.8 J kg^{-1}K^{-1}, $\Delta T_{ad,\,max}$ = 16 K). Additionally, the weak magnetic coupling in **2** make it maintain a considerable value of $-\Delta S_{m,max}$ at moderate field ($-\Delta S_{m,max}$ = 41.1 J kg^{-1}K^{-1} at ΔH = 3 T) and has a lower working temperature region. This observation indicates the importance of controlling not only large metal/ligand ratio but also weak magnetic interactions for successful design of molecular refrigerants.

Acknowledgements

This work was supported by the "973 Project" (2012CB821704 and 2014CB845602), project NSFC (Grant no. 91122032, 21371183, 21121061 and 21201137), the NSF of Guangdong (S2013020013002), Program for Changjiang Scholars and Innovative Research Team in University of China (IRT1298).

Notes and references

1 a) E. Warburg, *Ann. Phys*. 1881, **249**, 141; b) P. Debye, *Ann. Phys*., 1926, **386**, 1154; c) W. F. Giauque, *J. Am. Chem. Soc.*, 1927, **49**, 1864; d) W. F. Giauque and D. P. MacDougall, *J. Am. Chem. Soc*., 1935, **57**, 1175.

2 a) M. Evangelisti and E. K. Brechin, *Dalton Trans.*, 2010, **39**, 4672; b) M. Evangelisti, F. Luis, L. J. de Jongh and M. Affronte, *J. Mater. Chem.*, 2006, **16**, 2534; c) Y.-Z. Zheng, G.-J. Zhou, Z.-P. Zheng and R. E. P. Winpenny, *Chem. Soc. Rev.*, 2014, **43**, 1462; d) J.-L. Liu, Y.-C. Chen, F.-S. Guo, M.-L. Tong, *Coord. Chem. Rev.*, 2014, **281**, 26.

3 R. L. Carlin, *Magnetochemistry*, Springer-Verlag, Germany, 1986.

4 a) F. Torres, J. M. Hernández, X. Bohigas and J. Tejada, *Appl. Phys. Lett.*, 2000, **77**, 3248; b) X.-X. Zhang, H.-L. Wei, Z.-Q. Zhang and L. Zhang, *Phys. Rev. Lett.*, 2001, **87**, 157203.

5 a) F.-S. Guo, J.-D. Leng, J.-L. Liu, Z.-S. Meng and M.-L. Tong, *Inorg. Chem.*, 2012, **51**, 405; b) Y. Meng, Y.-C. Chen, Z.-M. Zhang, Z.-J. Lin and M.-L. Tong, *Inorg. Chem.*, 2014, **53**, 9052.

6 Y.-C. Chen, F.-S. Guo, J.-L. Liu, J.-D. Leng, P. Vrábel, M. Orendáč, J. Prokleška, V. Sechovský and M.-L. Tong, *Chem. Eur. J.*, 2014, **20**, 3029.

7 a) Y.-C. Chen, F.-S. Guo, Y.-Z Zheng, J.-L. Liu, J.-D. Leng, R. Tarasenko, M. Orendáč, J. Prokleška, V. Sechovský and M.-L. Tong, *Chem. Eur. J.*, 2013, **19**, 13504; b) L.-X. Chang, G. Xiong, L. Wang, P. Cheng, B. Zhao, *Chem. Commun.*, 2013, **49**, 1055; c) F.-S. Guo, Y.-C. Chen, L.-L. Mao, W.-Q. Lin, J.-D. Leng, R. Tarasenko, M. Orendáč, J. Prokleška, V. Sechovský, M.-L. Tong, *Chem. Eur. J.*, 2013, **19**, 14876; d) M. Wu, F. Jiang, X. Kong, D. Yuan, L. Long, S. A. Al-Thabaiti and M. Hong, *Chem. Sci.*, 2013, **4**, 3104; e) J. W. Sharples, Y.-Z. Zheng, F. Tuna, E. J. L. McInnes and D. Collison, *Chem. Commun.*, 2011, **47**, 7650; f) R. J. Blagg, F. Tuna, E. J. L. McInnes and R. E. P. Winpenny, *Chem. Commun.*, 2011, **47**, 10587; g) F.-S. Guo, Y.-C. Chen, J.-L. Liu, J.-D. Leng, Z.-S. Meng, P. Vrábel, M. Orendáč and M.-L. Tong, *Chem. Commun.*, 2012, **48**, 12219; h) J.-Z. Qiu, L.-F. Wang, Y.-C. Chen, Z.-M. Zhang, Q.-W. Li and M.-L. Tong, *Chem. Eur. J.*, 2015, **21**, DOI: 10.1002/chem.201503796.

8 a) M. Evangelisti, O. Roubeau, E. Palacios, A. Camín, T. N. Hooper, E. K. Brechin and J. J. Alonso, *Angew. Chem. Int. Ed.*, 2011, **50**, 6606; b) R. Sibille, T. Mazet, B. Malaman, M. François, *Chem. Eur. J.*, 2012, **18**, 12970; c) Y.-L. Hou, G. Xiong, P.-F. Shi, R.-R. Cheng, J.-Z. Cui and B. Zhao, *Chem. Commun.*, 2013, **49**, 6066; d) S.-D. Han, S.-H. Miao, S.-J. Liu, X.-H. Bu, *Inorg. Chem. Front.*, 2014, **1**, 549; e) Y. Yang, Q.-C. Zhang, Y.-Y. Pan, L.-S. Long and L.-S. Zheng, *Chem. Commun.*, 2015, **51**, 7317; f) Y.-C. Chen, J. Prokleška, W.-J. Xu, J.-L. Liu, J. Liu, W.-X. Zhang, J.-H. Jia, V. Sechovský and M.-L. Tong, *J. Mater. Chem. C*, 2015, **2**, DOI: 10.1039/c5tc02352a.

9 a) G. Lorusso, M. A. Palacios, G. S. Nichol, E. K. Brechin, O. Roubeau and M. Evangelisti, *Chem. Commun.*, 2012, **48**, 7592; b) G. Lorusso, J. W. Sharples, E. Palacios, O. Roubeau, E. K. Brechin, R. Sessoli, A. Rossin, F. Tuna, E. J. L. McInnes, D. Collison and M. Evangelisti, *Adv. Mater.*, 2013, **25**, 4653; c) Y.-C. Chen, Z.-S. Meng, L. Qin, Y.-Z. Zheng, J.-L. Liu, F.-S. Guo, R. Tarasenko, M. Orendáč, J. Prokleška, V. Sechovský and M.-L. Tong, *J. Mater. Chem. A*, 2014, **2**, 9851; d) L. Sedláková, J. Hanko, A. Orendáčová, M. Orendáč, C.-L. Zhou, W.-H. Zhu, B.-W. Wang, Z. M. Wang and S. Gao, *J. Alloys Compd.*, 2009, 425; e) G. Lorusso, M. A. Palacios, G. S. Nichol, E. K. Brechin, O. Roubeau and M. Evangelisti, *Chem. Commun.*, 2012, **48**, 7592; f) P. F. Shi, Y. Z. Zheng, X. Q. Zhao, G. Xiong, B. Zhao, F. F. Wam and P. Cheng, *Chem. Eur. J.*, 2012, **18**, 15086; g) S. Biswas, A. Adhikary, S. Goswami and S. Konar, *Dalton Trans*., 2013, **42**, 13331; h)

S.-J. Liu, J.-P. Zhao, J. Tao, J.-M. Jia, S.-D. Han, Y. Li, Y.-C. Chen and X.-H. Bu, *Inorg. Chem.*, 2013, **52**, 9163.
10 A. T. Skjeltorp, C. A. Catanese, H. E. Meissner, W. P. Wolf, *Phys. Rev. B*, 1973, **7**, 2062.
11 SHELXTL 6.10, Bruker Analytical Instrumentation, Madison, WI (USA), **2000**.
12 D. Casanova, M. Llunel, P. Alemany, S. Alvarez, *Chem. Eur. J.*, 2005, **11**, 1479.
13 A. C. Sudik, A. P. Côté, and O. M. Yaghi, *Inorg. Chem.*, 2005, **44**, 2998.
14 T. Rajeshkumar, S. K. Singh and G. Rajaraman, *Polyhedron*, 2013, **52**, 1299.
15 L. Cañadillas-Delgado, Ó. Fabelo, C. Ruiz-Pérez and J. Cano, *Magnetic Interactions in Oxo-Carboxylate Bridged Gadolinium(III) Complexes*, Nova publishing, Spain, 2010.
16 N. F. Chilton, R. P. Anderson, L. D. Turner, A. Soncini and K. S. Murray, *J. Comput. Chem.*, 2013, **34**, 1164.
17 a) A. Adhikary, J. A. Sheikh, S. Biswas and S. Konar, *Dalton Trans.*, 2014, **43**, 9334; b) A.-J. Hutchings, F. Habib, R. J. Holmberg, I. Korobkov and M. Murugesu, *Inorg. Chem.*, 2014, **53**, 2102; c) F. Yang, Q. Zhou, G. Zeng, G.-H. Li, L. Gao, Z. Shi and S.-H. Feng, *Dalton Trans.*, 2014, **43**, 1238.
18 a) V. K. Pecharsky, K. A. Gschneidner Jr., J. *Magn. Magn. Mater.* 1999, **200**, 44; b) M. Evangelisti and E. K. Brechin, *Dalton Trans.* 2010, **39**, 4672.

Journal Name

ARTICLE

TOC: Two 3D Gd(III)-based coordination polymers, $[Gd(glc)(Hglc)(H_2O)]_n \cdot nH_2O$ (**1**) and $[Gd(Hglc)_3]_n$ (**2**) are reported. The Gd-O-Gd bridging model in **1** leads to a stronger magnetic coupling than **2** in which only the Gd-OCO-Gd bridging model is oberved. The following MCE measurements indicates the weaker magnetic coupling in **2** make it perform a higher MCE than **1**, especially at the moderate fields ($-\Delta S_{m,max}$ = 41.1 J kg^{-1}K^{-1} and 24.8 J kg^{-1}K^{-1} for **1** and **2** respectively at ΔH = 3 T).